

# Quenching of High $p_\perp$ Hadron Spectra by Hadronic Interactions in Heavy Ion Collisions at RHIC

K. Gallmeister, C. Greiner and Z. Xu  
*Institut für Theoretische Physik, Universität Giessen,  
 Heinrich-Buff-Ring 16, D-35392 Giessen, Germany*

Typically the materialization of high energetic transverse partons to hadronic jets is assumed to occur outside the reaction zone in a relativistic heavy ion collision. In contrast, a quantum mechanical estimate yields a time on the order of only a few fm/c for building up the hadronic wavefunction for jets with typical transverse momenta of  $p_\perp \leq 10$  GeV as accessible at RHIC facilities. The role of possible elastic or inelastic collisions of these high  $p_\perp$  particles with the bulk of hadrons inside the fireball is addressed by means of an opacity expansion in the number of collisions. This analysis shows that the hadronic final state interactions can in principle account for the modification of the (moderate) high  $p_\perp$  spectrum observed for central collisions at RHIC.

PACS numbers: 25.75.+r, 12.38.Mh, 24.85.+p

Keywords: heavy ion collisions, jet quenching, energy loss, hadronic final state interaction

## I. MOTIVATION AND ESTIMATES

One of the major goals of the ongoing experiments at the Relativistic Heavy Ion Collider (RHIC) in Brookhaven National Laboratory is to find and probe for a temporarily occurring macroscopical state of deconfined quark-gluon matter. So far, especially hadronic abundancies have been experimentally thoroughly studied. Total hadron multiplicity measurements, however, do reflect mainly the chemical equilibration and possible hadronization processes of the late stages of the system, and do not deliver direct information on the early stage with maximum energy density and temperature, where a deconfined and highly excited state is generally expected to be formed. Still, one of the very interesting first results of the RHIC experiments is, that one has established a significant suppression of moderately high  $p_\perp$  hadrons produced in central  $A+A$  collisions compared to rescaled peripheral collisions or rescaled (and extrapolated)  $p+p$  collisions: The results for the lower center-of-mass energy of 130 AGeV [1, 2] and also the preliminary data for 200 AGeV [3] show a suppression factor  $R(p_\perp)$  of about  $\approx 1/5$  for pions with  $p_\perp \approx 5$  GeV, and hence state a clear hint for (probably various) nuclear medium effects at work.

The most popular explanation for this phenomenon is the onset of the occurrence of so called ‘jet quenching’, anticipated in [4]. The idea is, that a high energetic parton moving through a dense coloured (and deconfined) medium will loose considerable energy due to collisions and induced gluon radiation, and its final fragmentation will give rise to particles with considerable lower energies [5]. Hence, measurements of jets seem to offer a direct access to probe the early stage when the deconfined matter is very dense. As a present theoretical consensus, the dominant mechanism for energy loss is thought to be the nonabelian radiation of gluons based on pQCD by the energetic partons [6, 7]. As a result, the momenta of the jet partons are attenuated before hadroniz-

ing. One should internalize the word of caution, that this appealing picture of applying perturbative QCD calculations is strictly valid only for such high energetic jets with  $E > 10 \dots 20$  GeV [7]. And indeed, it has been found that the suppression pattern of the hard jets (with  $E > 10$  GeV) can show some significant dependence on the initial properties of the deconfined state [8].

A recent calculation based on the rather involved GLV formalism for a finite number of coloured collisions [9] does indeed provide a good agreement with the data. Still, though, a phenomenological opacity parameter has to be adjusted [10]. In this study already various other effects (the Cronin effect as well as a slight modification of the gluon distribution due to shadowing) have been phenomenologically incorporated. These effects do partly counteract and compete with the pure parton energy loss and thus do make a detailed analysis already more delicate [11, 12]. Contrary, the proposal was made that the observed spectra for central collisions show a significant  $m_\perp$  scaling, being a manifestation of a direct remnant of the initial gluons which were liberated from gluon saturated nuclear distribution functions [13]. Here any possible later interactions of the jets with the surrounding medium which might or should alter the distributions are completely discarded.

It has also been raised very recently, that in an ideal strong quenching picture the  $p_\perp$  spectrum of the high momentum hadrons is simply given by early ‘surface emission’ of the outer regions, where roughly half of the there produced jets can escape into the vacuum without passing through any medium [14]. It has to be verified, whether such an idealised scenario of complete absorption of energetic partons in matter can actually be achieved. The proposal bears resemblance to a similar geometrical picture for the production of another hard hadronic probe, the  $J/\Psi$ , being invoked much earlier for a possible explanation of the so called ‘anomalous’ suppression pattern observed in  $Pb+Pb$  collisions at CERN-SPS [15].

Typically, it is assumed in all the above referred descriptions that the partons do exit the collision region as

pointlike particles before finally fragmenting into a ‘jet’ of hadrons. We now will point out that this prejudice should be of major concern, being invalid for present settings at RHIC. The potential magnitude of the hadronization time (or, to be more precise, the time to build up the hadronic wavefunction) is based on a relativistic and simple quantum mechanical estimate [16] for light quark hadronic states

$$t_q^{\text{hadr}} \approx E R^2 \quad (1a)$$

or heavy quark meson states

$$t_Q^{\text{hadr}} \approx \frac{E}{m_Q} R \quad (1b)$$

Here  $E$  denotes the energy of the leading ‘parton’ or jet,  $R$  states the transversal size of the to be formed hadrons and  $m_Q$  is the mass of a heavy quark. Taking (1a) with the average radius of the pion  $R_\pi \approx 0.5 \text{ fm}$  or (1b) substituting  $m_Q$  by  $m_\rho$  for a  $\rho$  meson and taking  $R_\rho \approx 0.8 \text{ fm}$ , one has for the formation time a simple understanding given as

$$t_F \approx 1 \dots 1.2 (E / \text{GeV}) \cdot \text{fm}/c \quad (2)$$

Hence, for leading hadrons with moderately high  $p_\perp \leq 10 \text{ GeV}$  original point-like jet-partons have established already a complete nonperturbative, transversal wavefunction after traveling a distance in the vacuum of length being smaller or equal than 10 fm. Accordingly, the jets should, to a large fraction, materialize into hadrons still inside the expanding fireball, which has a transversal size of roughly

$$R(\tau) \approx 8 \text{ fm} + 0.5 \cdot \tau,$$

where  $\tau$  denotes the local proper time of the longitudinally (Bjorken like) and transversally expanding system with velocity  $v_t \approx 0.5c$ .

It is clear, though, that the parton cannot materialize into hadrons if it still resides in a deconfined phase. The dressing with a potential wavefunction and its subsequent fragmentation can only occur outside of deconfined matter, i.e. either in the hadronic system or in vacuum. The physics of hadronization out of a deconfined plasma for fast partons is not understood. Thus the estimate (2) should really be seen as a crude guess. The major fact we want to stress is that the final energetic hadrons (with a moderately high transverse momentum  $p_\perp$ ) observed at RHIC could well be realized as nearly fully established hadrons already inside the late stage hadronic fireball. If this is the case, these (pre-)hadrons will interact (by collisions) with the bulk hadronic matter making up the fireball [17]. This picture of potential late hadronic final state interaction bears again a close similarity to the one applied to explain the  $J/\Psi$  suppression pattern by either hadronic comovers [18] or by early hadronic string-like excitations as early comovers [19].

Referring to the phenomenology of colour transparency, the objects becoming leading hadrons will interact as (pre-)mesons with the surrounding low momentum mesons with a cross section of roughly  $\sigma(t) = \sigma_0 \cdot (t/t_F)$  as long as their wavefunction is not completely being built up [16].  $\sigma_0 \approx 10 \dots 20 \text{ mb}$  denotes the typical total (elastic plus inelastic) cross section of two mesons. Indeed, at lower energies for the collisions, there might be strong resonance contributions, which give rise to a much larger cross section. The density of hadrons in the late fireball changes from about  $1 \text{ fm}^{-3}$  down to  $0.1 \text{ fm}^{-3}$ . The mean free path of the ‘fast’ hadron is then estimated to be  $\lambda \approx 1 \dots 10 \text{ fm}$ . Accordingly, a few collisions  $L/\lambda = 0, 1, 2, 3 \dots$  should take place. The system is potentially rather opaque! In return, a strong degradation of the momenta of the leading hadrons will result. This states the major motivation for the present study.

Looking at the available center of mass energy for an individual collision for mesons at the same rapidity, even for a value of  $p_\perp = 10 \text{ GeV}$ , one gets a  $\sqrt{s} < 2 \text{ GeV}$ , if the target is a pion (assumed being locally) at rest. For a  $\rho$  as target, one has an invariant mass of above  $2.5 \text{ GeV}$  for particles with a transverse momentum larger than  $3 \text{ GeV}$ . This behaviour is depicted in Fig. 1. In any case, at such lower energies the dominant part of the collisions of the mesons or premesons with hadrons of the bulk system is nonperturbative and cannot be described by pQCD methods.

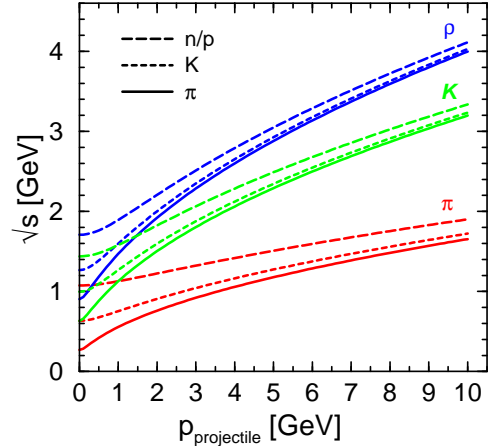


FIG. 1: The CMS energy for three targets at rest ( $\pi, K, \rho$ , depicted by the labels near the curves) and three types of projectiles ( $\pi, K, n/p$ , indicated by the solid, dashed and long dashed lines) as function of the momentum of the projectile.

For the considered transverse momentum region, one has either elastic scattering, resonance scattering or also inelastic scattering resulting in a few final hadrons. In section II we explain the description of the collision and introduce the notations of a folding matrix. Since the surrounding hadronic gas is expected to consist of approximately 40% (direct) pions, 10% kaons and 40% rhos, we treat in the following a typical inelastic collision within

the FRITIOF scheme [20] with a  $\rho$ -meson as characteristic target hadron being at rest. To also stress some model dependence, we compare with elastic scattering on a  $\pi$  as target particle, where the scattering is taken simply as isotropic. In section III we show various results for the transverse momentum spectra at midrapidity for various hadronic particles by assuming a definite number of undergone collisions. The initial spectra are hereby generated by the PYTHIA code. We end our discussion in section IV with a summary and some conclusions.

## II. ENERGY LOSS BY (MULTIPLE) FINAL STATE HADRONIC INTERACTIONS

Matter of interest are the transverse momentum spectra  $dN_i/dy d\vec{p}_\perp$ , where the index  $i$  stands for the various hadron species and the transverse momentum vector  $\vec{p}_\perp$  has to be taken as two dimensional. In all what follows, we will assume a Bjorken-like space-time picture with azimuthal symmetry, so that the only changes of the spectra from the two dimensional transverse momentum vector are given by its length  $p_\perp$  and we therefore will skip for reasons of simplicity all dependencies on the azimuthal angle.

In the framework of this assumption we are interested in particles lying in the same rapidity window, introducing the short hand notation  $f_i(p_\perp) \equiv dN_i/dp_\perp$  for this distribution function. (Our notation is different from the more common form  $dN_i/p_\perp dp_\perp$ , which is due to practical reasons in the descriptions presented below.) In order to separate these distributions of (hard) initial hadronic particles of type  $i$  from the dominant distributions of hadronic particles of type  $X$  with moderate or low (i.e. ‘soft’) momenta, say with  $p_\perp \leq 2$  GeV, we also do introduce the distribution functions  $\tilde{f}_X(p_\perp, \phi)$ . Here,  $\phi$  does not reflect the azimuthal angle in the cylindrical shaped Bjorken picture, but denotes the angle between the radial transverse direction and its actual momentum orientation. These latter distributions do describe the motion of the target particles. They are assumed to be steeply falling functions in the variable  $p_\perp$ , corresponding to a rather low temperature in a picture of ‘thermalized’ matter, superimposed by some collective, transversal (‘hydrodynamical’) flow.

Within these definitions, one can express the resulting spectrum of particles of the kind  $j$  after one collision of a (hard) particle of kind  $i$  with a (soft) target hadron of kind  $X$  as

$$f_j(p_\perp) = \sum_i \int dp_{\perp 0} f_i^0(p_{\perp 0}) \int dp_{\perp x} d\phi_x \tilde{f}_X(p_{\perp x}, \phi_x) \times g_{ij}^X(p_{\perp 0}; p_{\perp x}, \phi_x; p_\perp). \quad (3)$$

Here  $f_i^0(p_{\perp 0})$  has to be interpreted as the initial distribution of particle kind  $i$ , i.e. the distribution one would assume without any modifications. The ‘folding matrix’  $g_{ij}^X(p_{\perp 0}; p_{\perp x}, \phi_x; p_\perp)$  expresses the probability to get a

hadron of species  $j$  with momentum  $p_\perp$ , if a hadron of the species  $i$  and the transverse momentum  $p_{\perp 0}$  collides with a target hadron  $X$ , which is described by the transverse momentum component  $p_{\perp x}$  and the orientation  $\phi_x$ . Given this general structure with four independent variables,  $g_{ij}^X$  is a quite complicated object. It depends on the model employed for the collision (see below), and which is connected with the target, as indicated by the upper index.

Since the non-transversal component of the target momentum, which is encoded in the variable  $\phi_x$ , also leads to scattering in the longitudinal (beam) direction, equation (3) is, strictly speaking, only true if one assumes that scattering-out of a specified (tiny) region of rapidity is compensated by scattering-in from the next rapidity regions. This is the situation for the here assumed boost invariant Bjorken picture of 1-dimensional longitudinal expansion.

Setting in the following  $\tilde{f}_X(p_{\perp x}, \phi_x) = \delta(p_{\perp x}) \delta(\phi_x)$ , we assume for a general estimate that the low transverse momentum target is approximated by  $p_\perp \approx 0$ , which is reasonable, as long as the hard momentum scale is clearly separated from the low momenta of the bulk hadronic particles. This leads to the more simple and self-explanatory folding equation for momentum degradation

$$f_j(p_\perp) = \sum_i \int dp_{\perp 0} f_i^0(p_{\perp 0}) g_{ij}^X(p_{\perp 0}, p_\perp). \quad (4)$$

The basic problem is then effectively given by one-dimensional collisions. Here the reduced folding matrix  $g_{ij}^X(p_{\perp 0}, p_\perp)$  has a straightforward interpretation: It indicates the probability that out of a given particle  $i$  with transverse momentum  $p_{\perp 0}$  one gets a particle  $j$  with transverse momentum  $p_\perp$ , if the collision is taken with a target  $X$  at rest, where all this happens in the same rapidity interval. E.g. for elastic collisions  $i + X \rightarrow i + X$  ( $i \neq X$ ), one has the immediate normalization  $\int_0^\infty dp_\perp g(p_{\perp 0}, p_\perp) = 1$ .

Multiple, subsequent collisions are described by applying iteratively eq. (4), where in a new iteration step the distributions  $f_i^0$  have to be replaced by the  $f_i$  resulting from the former step.

We do remark some words of caution:

(1) The separation of the transversal distribution into a ‘hard’ contribution  $f_i$  and a ‘soft’ part  $\tilde{f}_X$  and setting the latter to a delta distribution implies some drawback, as this separation is artificial at low  $p_\perp$  (in the detector one would see  $f_i + \tilde{f}_i$ ) and thus leads to a ‘particle production’ effect at low values of  $p_\perp$ . This is connected with the normalization of the folding matrix  $g_{ij}^X$ , what one can see easily, if one for example looks at the simple situation of elastic scattering  $\pi^+$  on a  $\pi$ , i.e.  $i = \pi^+$  and  $X = \pi \equiv \frac{1}{3}(\pi^+ + \pi^0 + \pi^-)$ , leading to two pions with non vanishing transverse momenta. We remark here that one has to clearly stay in the discussion above a certain moderately large transversal momentum scale for an assumed clear separation of hard and low momentum scales.

(2) All our considerations assume, that a fixed number of collisions takes place, disregarding the fact, that the cross section could vary dramatically with the transverse momentum. For special collision partners, for example  $p + \pi$ , it is known [21], that the cross section  $\sigma_{\text{tot}}(p + [\pi^+ + \pi^-]/2)$  changes from  $\approx 30 \text{ mb}$  for  $p_{\text{proton}} = 3 \dots 6 \text{ GeV}$  to nearly five times this value at  $p_{\text{proton}} \approx 1.8 \text{ GeV}$ , if the pion is considered to be at rest. Similarly, the elastic reaction  $\pi + \pi \rightarrow \rho \rightarrow \pi + \pi$  also exceeds 100 mb for the projectile momentum  $p_\pi \approx 2 \dots 2.5 \text{ GeV}$ . This implies that, while assuming that one collision appears, at an other value of the transverse momentum (in these special cases) five collisions are to be awaited. We will comment on this point a little further in the conclusions.

### A. Initial distribution

For the initial distribution  $f_i^0$  of individual hadrons  $i$  at moderately high  $p_\perp$  when entering the final hadronic stage we do not have direct information. All various ideas, as mentioned in the introduction, might contribute and already steepen the spectrum. In order to see clearly the potential effect of the late hadronic interactions, we use individual distributions generated by PYTHIA v6.2 [22] gauged to individual  $p\bar{p}$ -collisions.

It is essential to carefully adjust the parameters for the model calculations to data provided by the UA1 collaboration for  $p\bar{p}$  collisions in the energy range  $\sqrt{s} \geq 200 \text{ GeV}$  and  $|y| < 2.5$  [23]. Fitting the calculations to the data, one gets a best description of the experimental results by just tuning one parameter, the intrinsic transverse momentum distribution of the partons inside the nucleon, described by its averaged value  $\langle k_\perp \rangle(\sqrt{s})$ . The resulting spectra are displayed in Fig. 2.

In a second step one has to compare the calculated spectra with the parametrization  $(1 + p_\perp/\bar{p}_0)^{-n}$  used to describe the experimental data [23] and extract from this fitted parametrization  $(\bar{p}_0(\sqrt{s})$  and  $n(\sqrt{s})$ ) the characteristic value  $\langle p_\perp \rangle(\sqrt{s})$ . With this knowledge one can extrapolate the calculations of  $p\bar{p}$  collisions down to the energy  $\sqrt{s} = 130 \text{ GeV}$  by adjusting the intrinsic parameter  $\langle k_\perp \rangle$  to finally meet the experimentally extrapolated value  $\langle p_\perp \rangle(\sqrt{s} = 130 \text{ GeV}) = 0.385 \text{ GeV}$  [23]. Please note that this value is completely disregarded by the assumed pointwise interpolation of fits to data from different values of  $\sqrt{s}$  for given transverse momentum  $p_\perp$ , as used eg. in [1, 24].

After having adjusted the microscopic Monte-Carlo calculations for  $p\bar{p}$  collisions at  $\sqrt{s} = 130$  and  $200 \text{ GeV}$  and  $|y| < 2.5$ , theoretical predictions for  $Au-Au$  collisions at these energies for midrapidity are given by respecting the correct isospin average corresponding to  $0.16 \cdot pp + 0.36 \cdot nn + 0.48 \cdot pn$ . It is worth noting, that these distributions do not follow a true power law behaviour, as can be seen in Fig. 3, where at  $p_\perp \simeq 2 \text{ GeV}$  and  $\simeq 6 \text{ GeV}$  significant changes in the slope occur.

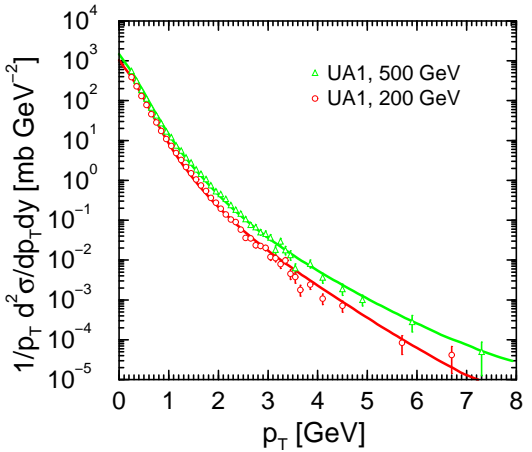


FIG. 2: Charged hadron distributions for  $p\bar{p}$  collisions calculated with PYTHIA at  $\sqrt{s} = 200, 500 \text{ GeV}$  compared with experimental data [23].

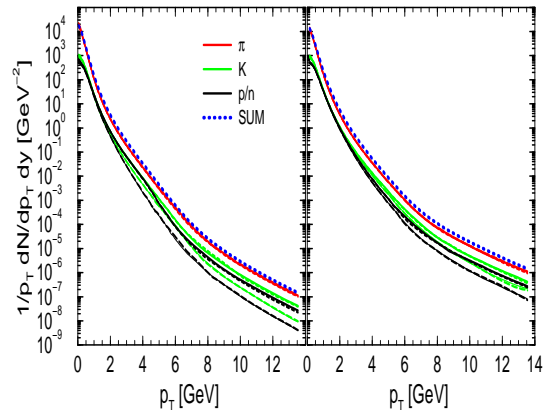


FIG. 3: Hadron distributions at midrapidity for  $Au-Au$  collisions at  $\sqrt{s} = 130 \text{ GeV}$  (left) and  $\sqrt{s} = 200 \text{ GeV}$  (right) calculated with PYTHIA. Pions, kaons and protons/neutrons are separated by line colour, while their charge state [negative (long dashed), neutral (solid), positive (dashed)] is indicated by the line style. Neutral anti-particles are displayed with a thin line. The sum of all charged particles is depicted by the thick dotted curve. Note that the spectra of all pions are similar and the spectra of neutral (anti)kaons and nucleons are similar to that of their positive (negative) charged partners.

Some special care has to be taken (for example mixing of calculations with non-weighted and some with reweighted events) to expand the PYTHIA Monte-Carlo calculations up to values of  $p_\perp$  larger than  $10 \text{ GeV}$  with best statistics. Naive Monte-Carlo implies, that at  $p_\perp \approx 6 \text{ GeV}$  reasonable computation time ends and that one would have to increase the number of events by approximately a factor of 10 every time one wants to go further in the  $p_\perp$  spectrum by an other step of  $2 \text{ GeV}$ , as one can see in Fig. 3.

## B. Folding Matrices

The collision of a high  $p_{\perp}$  particle with particles of the medium is implemented according eq. (4) via a folding matrix  $g_{ij}(p_{\perp 0}, p_{\perp})$ . Since a unique description of scatterings at these low energies (cf. Fig. 1) is not available, model descriptions have to be chosen.

In our first description A we calculate the folding matrices with Monte-Carlo calculations using the package FRITIOF [20] to simulate collisions with a  $\rho$ -meson. Since it is known, that within FRITIOF the relative weighting between elastic and inelastic scatterings is not in full agreement with data, we therefore choose a constant weighting according the ratio 15:85. (This is given by the averaging of  $p + \rho^-$ ,  $\pi + \pi^-$ ,  $K + \pi$  cross sections in a pomeron/reggeon exchange picture for  $\sqrt{s} > 2$  GeV and also following simple estimates in a constituent quark model.)

As a second description B we use purely elastic scattering on a pion, where the angular distribution of the outgoing particles in the cm system is assumed to be isotropic, which seems to be at a first glance a rather strong assumption.

In the description A of the collisions we are forced to extrapolate the FRITIOF prescription downwards to energies, where it is strictly not fully applicable anymore (for values below an initial transverse momentum of  $p_{\perp 0} \simeq 3$  GeV we are in the resonance region, cf. Fig. 1). Therefore (or nevertheless) we stop the calculations at a minimal initial transverse momentum of about  $p_{\perp 0}^{\min} = 1$  GeV. Boundary problems applying the folding procedure according eq. (4) due to this cut could be easily cured, if one implements a more detailed weighting of inelastic and elastic cross sections, which could already allow to bend the calculations downwards to zero transverse momentum, or if one would be able to introduce a consistent picture of scattering of hadrons from very low (resonance region) to very high momenta (hard QCD processes).

The two different model descriptions show some significant differences, if one looks at the dependence of the final transverse momentum  $p_{\perp}$  for a given initial transverse momentum  $p_{\perp 0}$ . But not only the different models, but also different final particles behave differently. This is shown in Fig. 4, where as an example the convolution matrices  $g_{i\pi^+/p^+}^{(\pi)}$  and  $g_{i\pi^+/p^+}^{(\rho)}$  are shown for the model descriptions A and B for the fixed value of the initial transverse momentum  $p_{\perp 0} = 5$  GeV.

While all the elastic distributions (Fig. 4 (bottom)) do follow a flat behaviour, where the threshold values are dictated by  $p_{\perp 0}$  and the corresponding masses of the particles, the inelastic distributions (Fig. 4 (top)) do possess a much richer structure. First they show, as expected, a strong enhancement at low  $p_{\perp}$  values. In addition, these curves also depict a double peak structure for the largest  $p_{\perp}$ -values in the forward scattering region. The lower peak at  $p_{\perp} = p_{\perp 0}$  is the simple one due to elastic scattering, while the second and rather astonishing peak

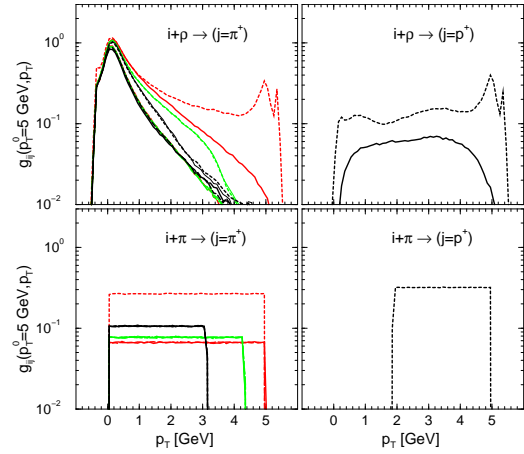


FIG. 4: The folding matrices  $g$  according (in)elastic scattering on a  $\rho$  (top) or elastic scattering on a  $\pi$  (bottom) for a  $\pi^+$  (left) and a  $p$  (right) as outgoing particle for a fixed value of the initial transverse momentum  $p_{\perp 0} = 5$  GeV as function of the resulting transverse momentum  $p_{\perp}$ . The line styles are chosen as in Fig. 3, indicating the different incoming particles. ‘Negative’ values for transverse momenta  $p_{\perp}$  stand for scattering in the opposite direction with positive momenta.

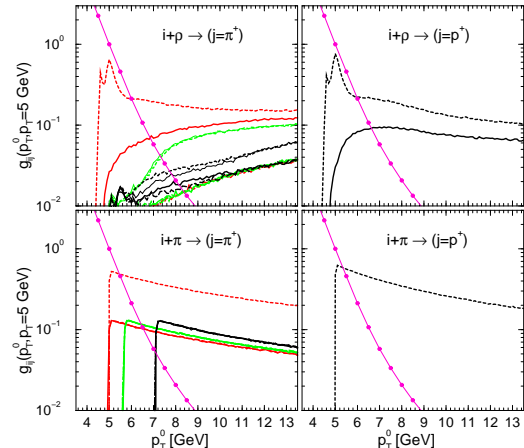


FIG. 5: As Fig. 4, but now as function of the initial transverse momentum  $p_{\perp 0}$  for a given resulting transverse momentum  $p_{\perp} = 5$  GeV. The connected dots stand for the slope of  $f_{(h++h-)/2}(p_{\perp 0})$  at  $\sqrt{s} = 200$  GeV.

for  $p_{\perp} > p_{\perp 0}$  is due to a large partial cross section for  $X + \rho \rightarrow X + \pi$  implemented in FRITIOF ( $X$  denotes here either the  $\pi^+$  in the upper left figure or the proton in the upper right one of Fig. 4). This peak is located at  $(p_{\perp} - p_{\perp 0}) \simeq (m_{\rho}^2 - m_{\pi}^2)(2m_{\rho}) \approx m_{\rho}/2$ . Physically, for such collision events the leading particles do become slightly accelerated. One might argue, that the likelihood of such contributions are completely overestimated, so that FRITIOF should also fail in this part of the description. On the other hand, by including them, their net effect in our later discussion would be that one actually

underestimates the emerging depletion of the transverse momentum spectrum. We have decided to omit these contributions from the inelastic part by hand compared to the basic FRITIOF concept.

Considering eq. (4), one realizes the fact that the behaviour of the folding matrices for a fixed value of the resulting transverse momentum  $p_\perp$  as a function of the initial transverse momentum  $p_{\perp 0}$  is of crucial importance. The corresponding figures for the examples from above are depicted in Fig. 5.

While the curves for the elastic scattering on a pion are smoothly falling for  $p_{\perp 0} \geq p_\perp$  (or the corresponding threshold value), the curves for the scattering on a  $\rho$  are nearly constant, but also showing the double peak structure at  $p_\perp = p_{\perp 0}$  and  $p_\perp > p_{\perp 0}$ , as mentioned above. For larger  $p_{\perp 0}$  the behaviour of all these folding curves gets less and less important for the final spectrum, since one has to fold them with the initial distribution, whose steep slope is also indicated in Fig. 5. This means that the correct way of looking at the stopping is the function  $g_{ij}(p_\perp = \text{const})$  instead of  $g_{ij}(p_{\perp 0} = \text{const})$ . Looking at the potential size of the energy loss (at a partonic or a hadronic level), the value  $p_{\perp 0} - p_\perp$  of  $g_{ij}(p_{\perp 0}, p_\perp)$  is strongly skewed toward small values by the steeply falling distribution  $f_i^0(p_{\perp 0})$ . Only the least stopped particles (i.e. particles with  $p_{\perp 0}$  only somewhat larger than  $p_\perp$ ) in  $g_{ij}$  contribute to the folding integral eq. (4). Simple estimates give, that values of  $g_{ij}$  with  $p_\perp < \frac{1}{2}p_{\perp 0}$  contribute only at a one percent level. Although appealing from the various shapes of the folding matrix  $g_{ij}$ , assumptions like  $\Delta E = \Delta p_\perp = \langle p_\perp - p_{\perp 0} \rangle \simeq \langle p_\perp \rangle \simeq \text{const} \cdot p_{\perp 0}$  for an averaged energy loss are much too oversimplistic.

These findings are in complete agreement with the considerations of [7], where the energy loss of (very energetic) partons in partonic matter due to gluon radiation, calculated via perturbative QCD, is expressed via a function  $D(\epsilon)$ , which has to be integrated in a sensible way with  $\epsilon$  as a measure of the energy shift.

Inspecting further Fig. 5, the  $p_\perp > p_{\perp 0}$  peak of the FRITIOF results will lead to some (maybe unphysical) “unstopping”, as already emphasized. As those contributions are indeed then weighted with the much larger distribution  $f(p_{\perp 0})$  at  $p_{\perp 0} < p_\perp$ , they would indeed be of more crucial importance than naively expected. Including those contributions would roughly weaken the deacceleration effect in the spectrum by a factor of 2 for  $p_\perp \geq 3$  GeV and lead to a zero net effect at  $p_\perp \simeq 2$  GeV. As already discussed, we will exclude these contributions with  $p_{\perp 0} < p_\perp$ .

### III. QUENCHING BY MULTIPLE COLLISIONS AND COMPARISON WITH DATA

Employing the appropriate scaling of binary collisions ( $N_{\text{coll}} = 945, 905, 19, 3.7$  for the centralities 0...5%, 0...10%, 60...80% and 80...92% respectively), the PYTHIA calculations are in perfect agreement with the

(at that time preliminary) PHENIX data [25] for charged hadrons and for neutral pions in the case of peripheral collisions, as can be seen in Figs 6 and 7. We can thus conclude that our PYTHIA calculation with the correct extrapolation provides an accurate basis for the experimental comparison.

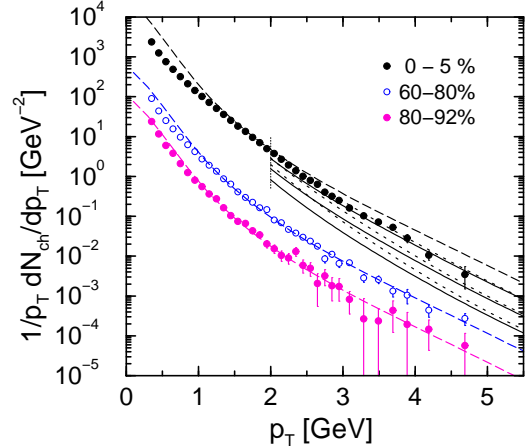


FIG. 6: Comparison of the calculations at midrapidity with the (at that time preliminary) PHENIX data [25] (but see also [1]) on charged hadrons for three different centralities. The thin dashed lines indicate the results from PYTHIA scaled with a corresponding binary collision number  $N_{\text{coll}}$ . The solid lines depict the spectra for the most central region, where the particles have suffered on average  $\langle L/\lambda \rangle \equiv 1, 2, 3$  (in)elastic hadronic collisions on a  $\rho$ , while the dotted lines indicate the same effect for elastic scattering on a  $\pi$ . These modifications are only shown for  $p_\perp > 2$  GeV.

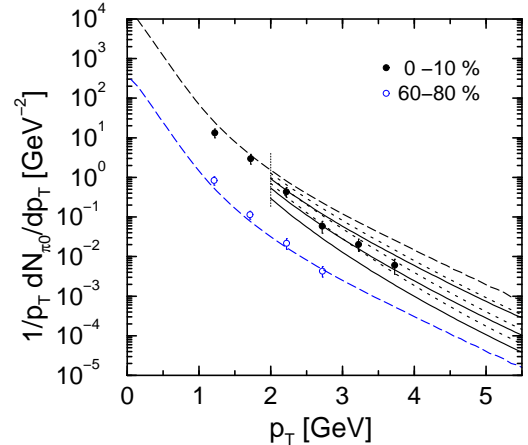


FIG. 7: As Fig. 6, but here a comparison with the PHENIX data [25] on  $\pi_0$  is depicted.

Looking at the most central data, one recognizes the celebrated significant discrepancy between our scaled PYTHIA results and the data. The data resides below the theoretical curve for  $p_\perp < 1.5$  GeV and for  $p_\perp > 2.5$  GeV. Only the latter case for  $p_\perp \geq 2$  GeV we now want to address by means of our scenario of possible (multiple)

collisions of the jet-like (pre-)hadrons with the ‘soft’ hadrons sitting in the bulk matter of the fireball. There is some general agreement that the hadron spectra below  $p_\perp \simeq 2$  GeV should be dominated by soft physics and hydrodynamical expansion with some appreciable collective outward flow. In addition, in this lower momentum regime our basic assumption of a hadronic target being approximately at rest becomes no more valid. Here not only energy loss, but probably also some collisional energy gain (on a partonic and/or hadronic level) and also hadronic particle annihilation and (re-)absorption occurs which influences the shape of the spectrum.

Referring to eq. (4) and inspecting the two Figs. 4 and 5, one recognizes that the depletion in the spectrum by one collision should be stronger for description A with (in)elastic collision on a  $\rho$  as the soft target particle, as one would also intuitively expect. This is so as the foldings matrices  $g_{ij}$  for  $p_{\perp 0} > p_\perp$  are somewhat smaller for this first collision picture, though there is the same strength at  $p_{\perp 0} \simeq p_\perp$ . In Figs 6 and 7 the three solid lines depict the spectrum (for  $p_\perp > 2$  GeV) for the most central region, when the particles have suffered on average 1,2,3 (in)elastic hadronic collisions on a  $\rho$ . The dotted lines in these figures indicate the effect for elastic scattering on a  $\pi$ . Indeed, for the inelastic case the overall depletion is somewhat stronger. Referring to our earlier remarks, we only do show the modifications for  $p_\perp > 2$  GeV. One clearly recognizes the potential importance of these possible final state interactions. For  $p_\perp > 2$  GeV an average loss with  $\langle L/\lambda \rangle = 1 \dots 2$  collisions are appropriate to explain the present experimental data both for charged hadrons and neutral pions.

We remark, that the potential energy loss by final state hadronic reactions is in the same range as considered in the various discussions for the jets in possible deconfined matter.

In Figs. 8 and 9 we now show calculations for various number of collisions at a  $\sqrt{s_{NN}} = 200$  GeV up to  $p_\perp = 10$  GeV. Our results might serve also as a guideline and prediction concerning the present analysis of the 200 GeV runs at RHIC [3]. In principle, the results are completely similar to the one carried out at the lower RHIC energies. Fig. 8 shows the resulting  $p_\perp$  spectra after 1,2,3 collisions according to the two collision pictures. As expected, the modification of the spectrum is similar to the one discussed for the situation at lower energies of  $\sqrt{s} = 130$  AGeV. Thus we can conclude that hadronic final state collisions are efficient in degrading the transverse energy of jet-like hadronic particles.

Fig. 9 gives the resulting suppression factor  $R(p_\perp) = \frac{dN/dp_\perp|_{\text{modified}}}{dN/dp_\perp|_{\text{initial}}}$  for collisions from Fig. 8. Here the effect of the different collision schemes is more visible. With one to two inelastic collisions one will have a suppression of 50 to 80 percent for momenta  $p_\perp \geq 4$  GeV.

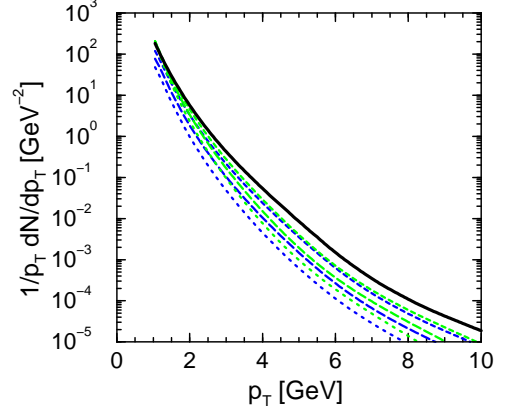


FIG. 8: Resulting  $p_\perp$ -spectra of charged hadrons at midrapidity for  $\sqrt{s} = 200$  GeV (solid black line) and for  $\langle L/\lambda \rangle \equiv 1, 2, 3$  (top to bottom) collisions according (in)elastic scattering on a  $\rho$  (blue) or elastic scattering on a  $\pi$  (green-light).

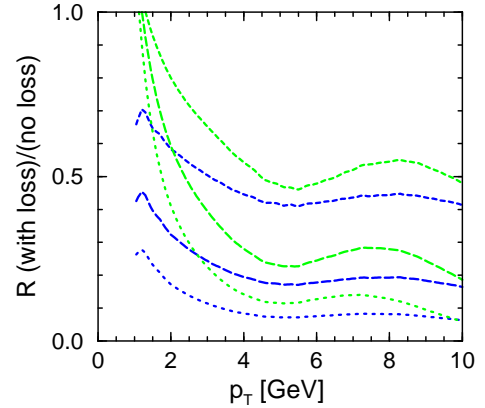


FIG. 9: The suppression factor  $R(p_\perp)$  of charged hadrons at midrapidity for  $\sqrt{s} = 200$  GeV for  $\langle L/\lambda \rangle \equiv 1, 2, 3$  (top to bottom) collisions according (in)elastic scattering on a  $\rho$  (blue) or elastic scattering on a  $\pi$  (green).

#### IV. SUMMARY

We have motivated that most of the (pre-)hadrons stemming from a jet should still materialize in the dense system for transverse momenta up to 10 GeV. The late hadronic final state interactions with the bulk of co-movers have a clear and nonvanishing effect in suppressing the spectrum. This is so for (in)elastic reactions on a  $\rho$ , which we have modelled via the FRITIOF scheme, and also for (isotropic) elastic scattering on a  $\pi$ . On the average one up to two such interactions should already be enough to explain quantitatively the RHIC results.

Although this comparison of the depletion of the spectra with real data is intriguing, one should be aware that our calculations are at best semi-quantitative. This is so because of a couple of simplifying assumptions invoked in the present study. We have neglected all possible de-

pendencies of the cross sections of the colliding “hard” and “soft” (target) particles, but do assume that a fixed number of collisions has taken place, following a simple-minded opacity expansion. In particular, possible resonance contribution for the elastic scattering could enhance the effect of momentum degradation considerably. Second we made the further assumption, that the bulk hadronic targets are taken at rest. This is certainly not the case especially if one wants to quantitatively discuss the modifications in the spectra around  $p_\perp = 1 \dots 3 \text{ GeV}$ , where both collective and ‘thermal’ dynamics should play a considerable role. Energy gain and loss mechanisms should both be at work and are probably competing in this momentum range. On a partonic level such a picture has been discussed in [26], but this should be rather obvious if one thinks of a kinetic cascade-type description either on a partonic or hadronic description of the dynamics happening inside the fireball. Hence, the marriage of a transport description for the ‘soft’ matter by some standard ultrarelativistic heavy ion cascade together with the present ideas carried out in this study is one possible way to further proceed in order to obtain more quantitative results. We will leave this as a future option. A first and rather exploratory investigation in this direction has already been mentioned some time ago [27].

Our emphasis is, however, at this stage to point out that, in order to draw some deductions for possible QCD effects of a deconfined QGP phase on the materializing jets, one has to disentangle these from the here investigated final state interactions, before definite conclusions on the importance of a potential dense partonic phase, or

any other effect, can really quantitatively be drawn. This is certainly true for the case of the jets to be observed at RHIC. (At future LHC experiments observable jets with much higher  $p_\perp$  could actually materialize outside the fireball.)

Combining specific energy loss formulae with fragmentation functions of quarks and gluons into hadrons can therefore only be understood as an extremely “effective” approach, since no conclusive answer about the relative strength of hadronic final state interactions can be extracted. The possible disentanglement, though, is very challenging and delicate. Some valuable information on the right “initial distribution” will be learned by  $d + Au$  experiments [12], eg. the size of possible shadowing and the Cronin effect. However, like the medium-induced gluon radiation the here discussed final state interactions with the late stage hadronic matter is a pure heavy ion effect. Here the  $p_\perp$ -dependence of the ‘suppression’ pattern might reveal possible differences, as for higher  $p_\perp$  the time of formation for the hadronic wavefunction of the leading hadrons of a jet and the colour transparency effect should suppress these final state interactions. But this is speculation at present.

### Acknowledgments

Stimulating discussions with R. Baier, W. Cassing, T. Falter, P. Jacobs, B. Kämpfer, U. Mosel and J. Nagle are gratefully acknowledged. This work has been supported by BMBF.

---

[1] K. Adcox et al. [PHENIX], *Phys. Rev. Lett.* **88**, 022301 (2002); K. Adcox et al. [PHENIX], *nucl-ex/0207009*.

[2] C. Adler et al. [STAR], *Phys. Rev. Lett.* **87**, 112303 (2001); C. Adler et al. [STAR], *nucl-ex/0206011*.

[3] various presentations at the Quark Matter 2002 conference, proceedings to be published in *Nucl. Phys. A*.

[4] J.D. Bjorken, FERMILAB-PUB-82-59-THY (unpublished); X.N. Wang, M. Gyulassy, *Phys. Rev. Lett.* **68**, 1470 (1992).

[5] X.N. Wang, *Nucl. Phys. A* **698**, 296 (2002).

[6] R. Baier, Y. Dokshitzer, A. Mueller, S. Peigné, D. Schiff, *Nucl. Phys. B* **483**, 291 (1997); *Nucl. Phys. B* **484**, 265 (1997).

[7] R. Baier, Y. Dokshitzer, A. Mueller, D. Schiff, *JHEP* **109**, 033 (2001).

[8] K. Gallmeister, B. Kämpfer, O. Pavlenko, *Phys. Rev. C* **66**, 014908 (2002).

[9] M. Gyulassy, P. Leval, I. Vitev, *Nucl. Phys. B* **571**, 197 (2000); *Nucl. Phys. B* **594**, 371 (2001);

[10] P. Leval, G. Papp, G. Fai, M. Gyulassy, G. Barnaföldi, I. Vitev, Y. Zhang, *Nucl. Phys. A* **698**, 631 (2002).

[11] S. Jeon, J. Jalilian-Marian, I. Sarcevic, *hep-ph/0207120*.

[12] I. Vitev, M. Gyulassy, *hep-ph/0209161*.

[13] J. Schaffner-Bielich, D. Kharzeev, L. McLerran, R. Venugopalan, *Nucl. Phys. A* **705**, 494 (2002)

[14] B. Müller, *nucl-th/0208038*.

[15] J.P. Blaizot, J.Y. Ollitrault, *Phys. Rev. Lett.* **77**, 1703 (1996).

[16] Y. Dokshitzer, V. Khoze, A. Mueller, S. Troyan, ‘Basics of perturbative QCD’, Editions Frontières (1991).

[17] K. Gallmeister, C. Greiner, Z. Xu, *nucl-th/0202051*, proceedings of the Int. Workshop XXX on Gross Properties of Nuclei and Nuclear Excitations (Hirschegg 2002).

[18] S. Gavin, R. Vogt, *Nucl. Phys. B* **345**, 104 (1990); W. Cassing, E. Bratkovskaya, *Nucl. Phys. A* **623**, 570 (1997).

[19] J. Geiss, C. Greiner, E. Bratkovskaya, W. Cassing, U. Mosel, *Phys. Lett. B* **447**, 31 (1999).

[20] H. Pi, *Comp. Phys. Commun.* **71** (1992), 173.

[21] K. Hagiwara et al. [PDG], *Phys. Rev. D* **66**, 010001 (2002).

[22] T. Sjöstrand et al., *Comp. Phys. Commun.* **135**, 238 (2001).

[23] C. Albajar et al. [UA1], *Nucl. Phys. B* **335**, 261 (1990).

[24] A. Drees, *Nucl. Phys. A* **698**, 331 (2002).

[25] W. Zajc et al. [PHENIX], *Nucl. Phys. A* **698**, 39 (2002).

[26] E. Wang and X.N. Wang, *Phys. Rev. Lett.* **87**, 142301 (2001).

[27] S.A. Bass, *Nucl. Phys. A* **661**, 205 (1999).